in power efficiency and speed. Neuromorphic processor architectures are optimized on a hardware level to run neural-network-based algorithms as fast and efficiently as possible [7]. Such architectures derive these benefits from the use of analog systems in which the computation is inherently tied to the physics of the device itself, rather than defined in software on a generalized digital architecture. Analog systems, however, must be engineered to control noise in such a way that the signals of interest are not corrupted by the processing itself, a task which arrays [3, 23], implement MACs directly while others, such as the WDM architecture analyzed in this paper, implement weights as individual units and perform all summation simultaneously.

Many applications involve multiplying a batch of vectors with the same matrix, such as running inference tasks with input data on a fixed (pre-trained) neural network classifier. This approach optimizes inference tasks for high bandwidth signals and low latency results. In such cases, it can be advantageous to design analog MAC units where input signals $\mathrm{x}(t)$ can be modulated on fast time scales and are multiplied by “fixed” weights w that only change on relatively-slow time scales. In general, reconfiguring optoelectronic weights takes significantly longer than their optical signal bandwidth capacity. Optical processors thus need to be codesigned at a system level with an electronic circuitry that optimizes the decomposition of matrix–vector multiplications into smaller vector–vector products while reducing the number of redundant computations [24].

2.2 Role of individual resonators

Resonator-based weights are specifically designed to take advantage of wavelength-division multiplexing (WDM), in which separate signals are encoded on optical carriers with nonoverlapping wavelengths. In optical communications, multigigahertz signals are modulated as amplitude or phase changes on a continuous-wave (CW) carrier traveling through a bus waveguide. With WDM, hundreds of CW carriers with unique wavelengths can coexist in a single waveguide without interfering with one another, effectively creating many independent information channels within a single physical channel. An array of resonators, usually

way that is not usually seen in large many-resonator PICs. Ultimately, compensating calibration and control techniques are required for practical deployment in either case. A discussion of the most common options for MZI-based PICs can be found in [39].

3.3 Definitions

Normalized Weights: For simplicity's sake, we introduce a normalized weight $\hat{\omega} \in [0, 1]$. Conversion between real weight ω (as measured by the analog summing element) and normalized weight can be accomplished via the equation:

$$\hat{\omega} = \frac{\omega - \omega_{\text{min}}}{\omega_{\text{max}} - \omega_{\text{min}}} \tag{2}$$

where ω_{max} and ω_{min} are the maximum and minimum weight values, respectively.

Bit Representation: Before defining error quantities such as accuracy, precision and resolution, sometimes it is useful to refer to them in units of 'bits'. For example, if the relative error of a measurement is 0.125, or 12.5%, we can also refer to it as 3 bits, because it takes three digits to represent that number in binary representation. More generally, if the error is $\epsilon \in (0, 1]$, the bit representation can be computed as $\epsilon\,(\text{bits}) = \log_2(1/\epsilon) \in [0, \infty)$. For example, as the measurement error goes to 0, we say that it has infinite precision.

Accuracy: In the context of resonator weight banks, accuracy refers to the systematic error between the commanded weight (denoted $\vec{w}$) and actual resulting weight vector (W($\vec{w}$), where W

Table 2: Simplified microresonator weight bank model, from actuation current (step 1) to resulting weight (step 4).

Step	Physical mechanism
1	**Joule heating:** $= {}_0 + \sum^{N} \mathrm{K} \quad I^2$: local temperature; ${}_0$: room temperature; **K**: effective thermo-optic coefficient matrix (diagonal in the absence-48.016 -.84).

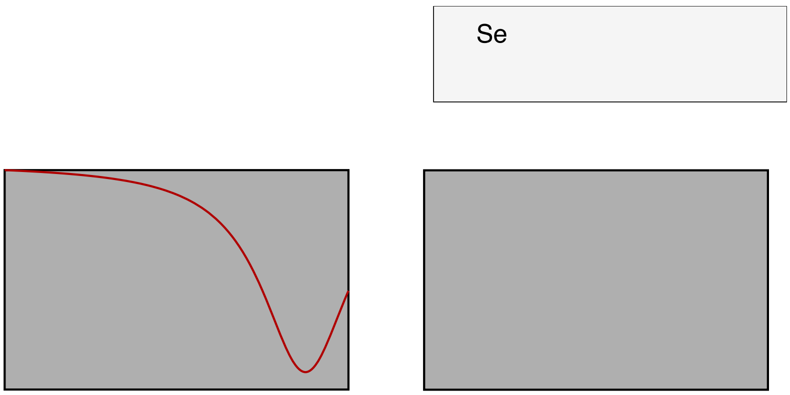
Se

5.3 Feedback control

[60] L. Chrostowski, X. Wang, J. Flueckiger, Y. Wu, Y. Wang, and S. T. Fard, ‘‘Impact of fabrication non-uniformity on chip-scale silicon photonic integrated circuits,’’ in